

# Vpliv kavitacijskih struktur na erozijo na simetričnem krilu v kavitacijskem predoru

## The Influence of Cavitation Structures on the Erosion of a Symmetrical Hydrofoil in a Cavitation Tunnel

Brane Širok - Matevž Dular - Matej Novak - Marko Hočevar -  
Bernd Stoffel - Gerhard Ludwig - Bernd Bachert

*Izvedena je bila vizualna in erozijska študija kavitacije na dvodimenzionalnem krilu v kavitacijskem predoru. Razvita je bila nova metoda vrednotenja kavitacijskih poškodb, ki temelji na računalniški vizualizaciji.*

*Z računalniško vizualizacijo je bila izvedena analiza kavitacijskih dogodkov nad krilom. Razvit je bil empirični model, ki povezuje moč kavitacijske erozije na površini krila in kavitacijske dogodke nad krilom. Empirični model omogoča opazovanje kavitacije v turbinskih strojih. Študija je del petega okvirnega evropskega projekta "Cavismonitor".*

© 2002 Strojniški vestnik. Vse pravice pridržane.

**(Ključne besede: kavitacija, erozija, vizualizacija računalniško podprta, modeli empirični)**

*A study of the visual and erosion effects of cavitation was performed on a two-dimensional hydrofoil in a cavitation tunnel. A new method of erosion-damage evaluation was developed, based on computer-aided visualization.*

*Using computer-aided visualization, a statistical evaluation of the cavitation structures above the hydrofoil was made. An empirical model was developed that relates the intensity of cavitation erosion on the hydrofoil surface and the visual structures of the cavitation above the hydrofoil. An empirical model enables monitoring and control of cavitation in turbo-machinery. The study is a part of the European 5<sup>th</sup> Framework Project "Cavismonitor".*

© 2002 Journal of Mechanical Engineering. All rights reserved.

**(Keywords: cavitation, erosion, computer-aided visualization, empirical models)**

### 0 UVOD

Kavitacija v hidravličnih strojih povzroča nihanje, povečanje hidrodinamičnega upora, spremembe hidrodinamike toka, hrup, termične, svetlobne učinke in erozijo. Vsi učinki kavitacije povzročajo hidravlične izgube v pretočnem delu in zmanjšujejo moč in učinkovitost strojev. Naš namen je povezati vidne kavitacijske dogodke nad krilom v kavitacijskem predoru z erozijo na površini. V prispevku bo predstavljena povezava med časovno in prostorsko odvisnimi topološkimi strukturami in kavitacijsko erozijo na krilu.

Pojav kavitacije je tesno povezan z lokalnimi časovno spremenljivimi hidrodinamičnimi lastnostmi kakor sta lokalna kinetična energija toka in lokalni statični tlak. V primeru, da lokalni statični tlak pade pod vrednost pripadajočega uparjalnega tlaka kapljevine, se v opazovanem področju oblikuje dvofazni tok kapljevine in pare, ki v področju povečanega statičnega tlaka prek kondenzacije pare preide v enofazni kapljevinski tok. Ta pojav spremljajo tlačni utripi.

### 0 INTRODUCTION

When cavitation occurs in hydraulic machines it produces vibrations, increases the hydrodynamic drag, changes the flow hydrodynamics, produces noise, thermal and light effects, and most importantly, it causes cavitation erosion. All cavitation effects generate hydraulic loss in the flow tract and decrease the machine's efficiency and power. The purpose of this paper was to relate the visible cavitation structures above a single hydrofoil in a cavitation tunnel with the erosion on the hydrofoil's surface. A functional relationship between the visible space and time-dependent topological structures and the cavitation erosion on the surface of a hydrofoil will be presented.

The cavitation phenomenon is related to local time-dependent hydrodynamic characteristics such as the local kinetic energy of the flow and the local ambient pressure. In the cases where the local ambient pressure drops below the vapour pressure, a two-phase flow of liquid and vapour is formed, which transforms to a one-phase liquid flow in a region where the pressure is higher than the condensation pressure. This phenomenon is accompanied by significant pressure pulsation.

Metode raziskav kavitacije delimo na celovite in lokalne metode. Celovite metode temeljijo na energijskih razmerjih. Celovite metode so v celoti standardizirane in podprte z mednarodnimi priporočili. Uporabljajo se pri prevzemnih preskusih na modelih hidravličnih strojev, npr. vodnih turbin, vijakov in črpalk. Z lokalnimi metodami obravnavamo kavitacijo časovno in prostorsko. Med lokalne metode prištevamo računalniško vizualizacijsko metodo, merjenje akustične emisije ter merjenje nihanja mehanskih sestavov in utripov tlaka v pretočnem delu. Lokalne metode so namenjene predvsem kot dopolnilo celovitim metodam.

V nasprotju s študijo kavitacije v hidravličnih strojih potekajo temeljne raziskave kavitacije na hidrodinamičnih krilih v kavitacijskih predorih. Namenjene so ugotavljanju novih empiričnih odvisnosti, ki so usmerjene predvsem v napoved erozijskih učinkov na stenah pretočnega dela ([1] in [2]).

## 1 KAVITACIJA

Kavitacijo delimo glede na obliko kavitacijskih pojavov v tekočini, glede na stopnjo ali režim kavitacije in glede na vzroke za nastanek kavitacije ([1] in [3]). Po obliki delimo kavitacijo na kavitacijo ločenih mehurčkov, kavitacijo v obliki žepa ali kavitacijskega oblaka in vrtnično kavitacijo, ki nastaja na mestih velike obročne napetosti v tekočini. Z vidika kavitacijske erozije na hidravličnih strojih je najpomembnejša kavitacija v obliki žepa ali kavitacijskega oblaka, katerega kavitacijski mehurčki implodirajo nad trdno površino rotorskih lopatic stroja [1].

Množico lastnosti, ki vplivajo na nastanek, razvoj in vrsto kavitacije, delimo na hidravlične in geometrične lastnosti. Med hidravlične lastnosti sodijo hitrost, spremembe hitrosti, tlak in spremembe tlaka. Med geometrične lastnosti prištevamo obliko, usmerjenost in hrapavost telesa. Poglavitne značilnosti kavitacijskega stanja v odvisnosti od hidravličnih razmer toka opišemo z brezdimenzijskim kavitacijskim številom  $\sigma$ , ki vključuje primerjalni tlak  $p_\infty$ , tlak uparjanja kapljevine  $p_v$  in hitrost toka  $v_\infty$  [1].

Z uporabo kavitacijskega števila  $\sigma$  lahko opišemo kavitacijske razmere toka tekočine glede na razmere brez kavitacije, začetno stopnjo kavitacije in kavitacijo v različnih fazah. Z zmanjšanjem kavitacijskega števila  $\sigma$  se povečuje kavitacijska ogroženost. Poleg povečane hitrosti toka in zmanjšanja statičnega tlaka v tekočini vplivajo na kavitacijo tudi geometrijske značilnosti kot so ostri robovi obtakanega telesa, povečanje vpadnega kota

Cavitation is studied using integral and local methods. Integral methods are based on energy effects that are standardised and supported by international recommendations. Integral methods are used during the model testing of hydraulic machines like water turbines, propellers and pumps. Using local methods, information about the space and time behaviour of cavitation in hydraulic machines is obtained. Local methods are computer-aided visualization methods and measurements of the acoustic emissions and vibrations of mechanical structures. Local methods are mainly used as a supplement to integral methods.

In contrast to studies of hydraulic machines, basic studies of cavitation are performed on hydrofoils in cavitation tunnels. The goal of these studies is to set new empirical relations, mainly predicting the erosion effects on the walls of flow tracts. Visualization studies confirm a relationship between material erosion and the type of cavitation, which is characterised by the dynamics and geometrical structure of the vapour cloud above the surface ([1] and [2]).

## 1 CAVITATION

Cavitation can be classified with regard to the shape of the cavitation structure in a fluid, to a stage or regime of cavitation, or according to its origin ([1] and [3]). With regard to the shape, cavitation can be classified as the cavitation of isolated bubbles, cavitation in the shape of a vapour pocket or to cloud cavitation and vortex cavitation, which appears at a location with high circumferential fluid tension. When observing the cavitation erosion of hydraulic machines, it is the shape of the vapour pocket or cloud cavitation that is the most important type. In the former case, cavitation bubbles implode above the solid surface of the rotor blades [1].

Parameters that have an influence on the appearance, growth and type of cavitation can be divided into hydraulic and geometrical parameters. The hydraulic parameters are flow velocity, velocity fluctuations, pressure, and pressure pulsations. The geometrical parameters are shape, orientation and roughness of an object. The basic properties of the cavitation condition as a function of the hydraulic conditions of flow are described with a non-dimensional cavitation number  $\sigma$ . This number includes the reference pressure  $p_\infty$ , the vapour pressure  $p_v$  and the flow velocity  $v_\infty$  [1]:

$$\sigma = \frac{p_\infty - p_v(T_\infty)}{\rho v_\infty^2 / 2} \quad (1)$$

With the aid of the cavitation number  $\sigma$  one can describe the cavitation conditions of fluid flow for non-cavitating flow, cavitation start-up and cavitation at different stages of development. When the cavitation number  $\sigma$  decreases, the cavitation aggressiveness increases. Besides increased velocity and decreased static pressure of the fluid flow, geometrical parameters such as sharp edges, increased inclination angle and roughness of the surface of the submerged body also

in povečana hrapavost površine. Hrapavost in nepravilnosti na površini telesa lahko delujejo kot viri kavitacijskih jeder.

Najpogostejša nezaželena posledica kavitacije je erozijska poškodba materiala, povzročena pri imploziji kavitacijskih mehurčkov v bližini trdne površine. Problem erozije materiala so intenzivno raziskovali že mnogi avtorji ([4], [5], [8] in [9]). Kolaps kavitacijskega mehurčka je proces, ki dela motnje in šoke z velikimi tlačnimi amplitudami v točki kondenzacije mehurčka. Če se ta dogodek odvija blizu trdne stene, nastanejo velike lokalne mehanske obremenitve v sestavi materiala. Ponavljanje te obremenitve zaradi množice mehurčkov, ki implodirajo, povzroča utrujanje materiala in »razkrajanje« materialne sestave na površini. Kakovostne študije dinamike kavitacijskih oblakov nakazujejo, da je kolaps mehurčkov v kavitacijskem oblaku agresivnejši od kolapsa posameznih mehurčkov [2]. Tlačna motnja nastane v trenutku, ko kavitacijski mehurčki v oblaku implodirajo in s tem povzročijo udarni val, ki se širi na vse strani. Če udarni val trči ob bližnjo steno, povzroči na njej močan tlačni udar velikosti nekaj deset MPa [4]. Velikost tega udara je primerljiva z mejo elastičnosti materiala. Drugi možni tip kavitacijske erozije se odvija z implozijo mehurčkov v neposrednem stiku s trdno steno v pretočnem delu. V tem primeru vpliva trdna površina na krogelno obliko mehurčka, ki postane nestabilen v svoji obliki. Opazovanja so pokazala, da lahko tako nastala asimetrija pri prehodu v področje z večjim tlakom zavzame obliko pospešenega curka kapljevine, usmerjenega skozi mehurček proti trdni steni [4]. Tako imenovani povratni mikrocurk (sl. 1) doseže veliko lokalno hitrost, ki povzroči udarni šok z veliko lokalno obremenitvijo materiala ([1] in [3]). V nadaljevanju se bomo usmerili predvsem v študijo mehanizma kolapsa množice mehurčkov v kavitacijskem oblaku, ki se s celovitimi parametri, to sta kavitacijsko število  $\sigma$  in vpadni kot na lopatico  $\delta$ , spreminja po obliki in kinematiki kavitacijskega oblaka.

## 2 PRESKUS

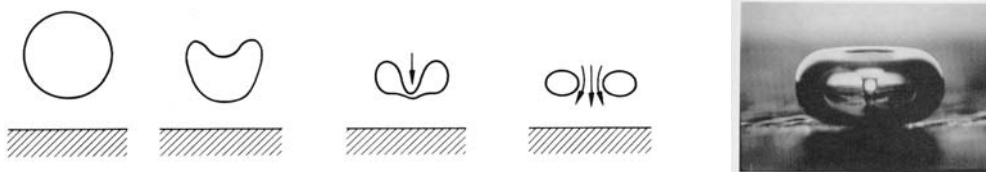
Ekspperimentalno delo je obsegalo študijo kavitacije na simetričnem krilu v zaprtem kavitacijskem predoru. Delo je potekalo na Tehniški univerzi v Darmstadtu – v Laboratoriju za turbinske stroje in

have an influence on cavitation aggressiveness. Roughness and unevenness of the surface of the body can act as a generator of cavitation cores.

The most unwanted consequence of cavitation is erosion damage, which is caused by bubble implosion near the solid surface of a body. Cavitation erosion has been studied by many authors ([4], [5], [8] and [9]). Bubble implosion is a process that generates disturbances and shocks with high amplitudes of pressure in the position of a bubble's condensation. If this process occurs close to a solid surface, high local mechanical tensions in the structure of the material are generated. Repeated disturbances, caused by numerous bubble implosions, results in fatigue and damage to the material's structure. Qualitative studies of cavitation clouds' dynamics show that the collapse of bubbles in a coherent cavitation cloud is more aggressive than the collapse of a group of single bubbles [2]. A pressure disturbance occurs when cavitation bubbles in a cavitation cloud implode and generate a shock wave that propagates in all directions. If the shock wave collides with a nearby surface it causes a large pressure shock of the order of several 10 MPa [4]. The magnitude of the shock is comparable to the elastic limit of the material. The second possible type of cavitation erosion happens when bubbles implode onto the solid surface of a flow tract. The solid surface of the body acts on the spherical shape of the bubble, which becomes unstable. Investigations have shown that the developed asymmetry at the transition into the region of higher pressure takes the form of an accelerated fluid micro-jet, directed through a bubble towards the solid surface [4]. The so-called reverse micro-jet (Fig. 1) can reach a high local velocity, which causes a shock with high local tension of the material ([1] and [3]). In addition, the study will focus on the implosion mechanism of a group of bubbles in a cavitation cloud, which changes its kinematics and shape in accordance with integral parameters such as the cavitation number  $\sigma$  and the blade inclination angle  $\delta$ .

## 2 EXPERIMENT

The experimental work included a cavitation study using a symmetrical hydrofoil in a closed cavitation tunnel of the Technical University Darmstadt, Laboratory for Turbomachinery and Fluid



Sl. 1. *Mehanizem nastanka mikrocurka in slika mikrocurka*[1] in [2]  
Fig. 1. *Mechanism of micro-jet generation and a picture of a micro-jet* [1] and [2]

tekočinsko energetiko in na Turboinštitutu v Ljubljani. Kavitacijski preskus na simetričnem krilu je bil izveden na kavitacijskem predoru na Univerzi v Darmstadtu, kjer je bila opravljena tudi eksperimentalna analiza erozijskih poškodb na izbranih mestih površine krila. V izbranih delovnih točkah so bile posnete zaporedne digitalizirane slike topoloških sestavov kavitacijskih oblakov. Predprocesirano vizualizacijsko gradivo je bilo analizirano s programsko opremo na Turboinštitutu v Ljubljani. V sklepnem delu preskusa je bila opravljena večparametrična analiza erozije v odvisnosti od moči in lege kavitacije.

## 2.1 Kavitacija na simetričnem krilu v kavitacijskem predoru

Pri preskusu je bilo uporabljeno simetrično krilo (sl. 2) s polkrožnim vpadnim robom dolžine 107,9 mm, širine 50 mm in debeline 16 mm. Kot primerjalna izmera je bila uporabljena debelina krila  $h = 16$  mm. Oblika krila z ravnimi vzporednimi stenami je bila izbrana zaradi tehnologije vrednotenja erozije na nadzornih površinah – vzorcih.

Krilo je bilo nameščeno v kavitacijskem predoru (sl. 2) s sklenjenim obtokom, tako da je bilo mogoče spreminjati tlak in imensko hitrost (kavitacijsko število –  $\sigma$ ) v sistemu. Srednja hitrost v testni ravnini pred krilom je znašala  $v = 16$  m/s, kar ustreza Reynoldsovemu številu  $Re = 256000$ . Med preskusom se je spreminjal podtlak v sistemu in vpadni kot krila  $\delta$  v mejah od  $0^\circ$  do  $7,5^\circ$ .



Sl. 2. Krilo in preskuševališče  
Fig. 2. Hydrofoil and test rig

Power, and analyses at the Turboinstitut Ljubljana. The cavitation experiment on the symmetrical hydrofoil, as well as the experimental analysis of the erosion damage at specific locations on the hydrofoil, was performed at the University of Darmstadt. Successive images of topological structures of the cavitation clouds were captured at selected operational points. Pre-processed visualization material was analysed with the aid of software at the Turboinstitut Ljubljana. In the final part of the experiment a multi-parametric analysis of cavitation erosion versus the magnitude and position of cavitation was performed.

## 2.1 Cavitation on a symmetrical hydrofoil in a cavitation tunnel

The experiment was performed on a symmetrical hydrofoil (Figure 2) with a circular leading edge. The hydrofoil was 107.9-mm long, 50-mm wide and 16-mm thick. The thickness of the hydrofoil ( $h = 16$  mm) was used as a reference dimension. The shape of the hydrofoil with parallel walls was applied to suit a method for the evaluation of cavitation erosion on control surfaces (samples).

The hydrofoil was placed in a closed-circuit cavitation tunnel (Figure 2) so that the system pressure and nominal velocity (cavitation number  $\sigma$ ) could be changed. The average velocity in front of the hydrofoil was constant ( $v = 16$  m/s) at  $Re = 256000$ . During the experiment the system pressure and inclination angle  $\delta$  (from  $0^\circ$  to  $7.5^\circ$ ) were modified.



Na krilu so bili nameščeni štiri valjni vzorci na mestih, ki jih prikazuje slika 2. Kavitacijsko število se je spreminjalo z nastavljanjem podtlaka v kavitacijskem predoru tako, da je bil vstopni rob kavitacijskega oblaka nad določenim vzorcem na krilu. Izbrana so bila štiri kavitacijska števila za vsak vpadni kot krila  $\delta$ . Integralne preskusne karakteristike so podane v preglednici 1.

Four specimens were placed in a hydrofoil, as shown in Figure 2. The cavitation number was set by changing the system pressure so that the leading edge of the cavitation cloud was located above a specific specimen on the hydrofoil. Four different cavitation numbers were chosen for each inclination angle. The integral experimental characteristics are shown in Table 1.

Preglednica 1. Kavitacijsko število v odvisnosti od vpadnega kota krila in mesta najintenzivnejše kavitacije  
Table 1: The dependence of the cavitation number on the hydrofoil inclination angle and the position of maximum cavitation

$\delta$	$\sigma_1$	$\sigma_2$	$\sigma_3$	$\sigma_4$
$0^\circ$	1,59	1,38	1,22	1,16
$2,5^\circ$	2,35	2,03	1,75	1,63
$5^\circ$	3,25	2,71	2,43	2,19
$7,5^\circ$	4,00	3,38	2,98	2,73

## 2.2 Ocenjevanje erozijskih učinkov kavitacije

Ocenjevanje erozijskih poškodb temelji na vrednotenju geometrijskih sprememb na površini vzorca. Vzorci so bili v krilo vstavljeni poravnano s površino in izpostavljeni toku (slika 2). Čas preskusa je bil 30 minut. Spremembe so se pokazale kot luknjice na površini valjnih vzorcev, ki so posledica erozije zaradi kavitacije. Pri preskusu smo uporabili vzorce premera 10 mm, narejene iz čistega bakra (sl. 3). Baker je primeren material zaradi mehanskih lastnosti, predvsem zaradi majhne trdote in majhne odpornosti na tlačne sunke, ki jih povzroči kavitacija. Luknjice na površini vzorca imajo premer velikostnega reda  $10^{-5}$  m.

Moč erozijskih učinkov kavitacije je bila določena s štetjem luknjic. Sistem za vrednotenje erozije je sestavljen iz mikroskopa, digitalne (CCD) kamere ter vira svetlobe (sl. 3). Razvit je bil program vrednotenja, ki luknjice prešteje in oceni njihovo površino. Občutljivost vrednotenja oziroma velikost nadzornega elementa sta bili nastavljivi. Najboljši rezultati so bili dobljeni pri velikosti nadzornega elementa  $18 \mu\text{m}$ , kjer področje – velikost nadzornega elementa ravno zajame luknjico povprečne velikosti. Program je upošteval prekrivanje dveh ali več luknjic. Da bi dobili reprezentativen nabor podatkov, je treba ovrednotiti dovolj veliko površino vzorca.

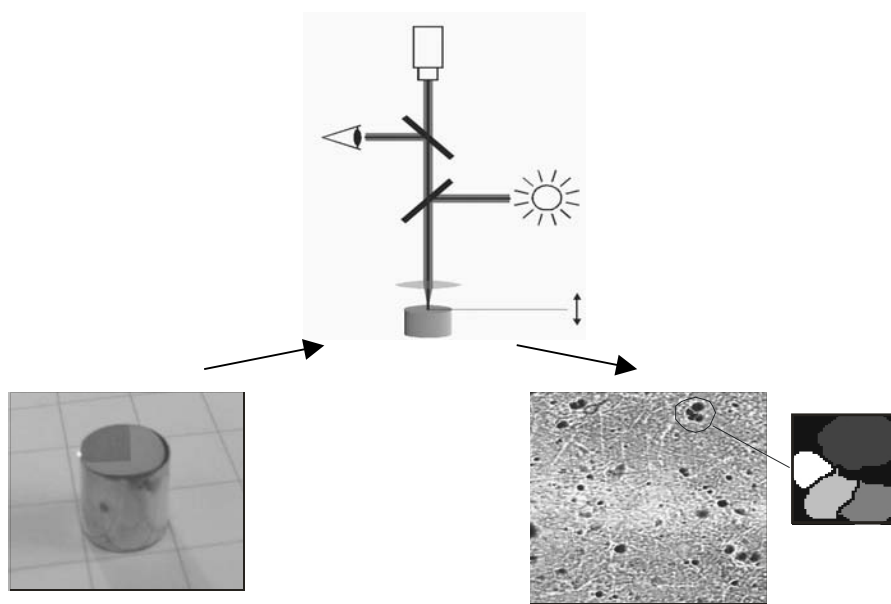
Količinska ocena poškodb kavitacijske erozije z metodo štetja luknjic je predstavljena v preglednici 2. Moč kavitacije količinsko podajata število  $N$  in površina luknjic  $A_d$ . Uporabljena metoda omogoča relativno medsebojno primerjavo vzorcev na krilu.

## 2.2 The method for evaluating cavitation erosion

The erosive aggressiveness of the cavitation condition can be quantified by the so-called pit-count method, i.e. a quantitative evaluation of the pits that are generated on the surface of a specimen. The specimens were mounted flush with the surface of the hydrofoil and exposed to cavitation (Figure 2). The exposure time was 30 minutes. Erosion effects are expressed as pits on the surface of the specimen. In the experiment, cylindrical specimens of 10-mm diameter, made with pure copper, were used (Figure 3). Pure copper is well suited because of its mechanical quantities, especially its low hardness, i.e. its low resistance to pressure shocks caused by cavitation. The pits have a diameter of  $10^{-5}$  m order of magnitude.

The number and size of the pits in relation to the cavitation exposure time and the type of material gives us a quantitative measure of the erosive aggressiveness. The system for recording the pits consists of a microscope, a CCD camera, and an illumination source (Figure 3). Image-processing software was developed to determine the aggressiveness of the erosion by counting the number of pits and determining their size. The sensitivity of the evaluation, i.e. the magnitude of the control element, is optional. Investigations have shown that a control element with a diameter of  $18 \mu\text{m}$ , where the control element covers a pit of average magnitude, offered the most plausible results. The software also considered the overlapping of two or more pits. In order to obtain a representative set of data, an appropriate surface area needs to be considered.

The quantitative evaluation of the cavitation erosion of the hydrofoil surface obtained by the pit-count method is shown in Table 2. The number ( $N$ ) and the pit area ( $A_d$ ) represent quantitative measures of the cavitation aggressiveness. The pit-count method allows a relative comparison of the specimens.



Sl. 3. Sistem za vrednotenje kavitacijske erozije  
Fig. 3. System for evaluating cavitation erosion

Preglednica 2. Podatki o poškodbah vzorcev pri strmini  $5^\circ$  (brez erozije na prvem vzorcu)  
 Table 2. Specimen erosion data for an inclination angle of  $5^\circ$  (with no erosion on the first specimen)

$\sigma$ / specimen	$A_{ref}$ mm <sup>2</sup>	$A_d$ mm <sup>2</sup>	$N$
3,25 / 1.	-	-	-
2,71 / 2.	24,75	1,64	2752
2,43 / 3.	24,53	1,14	2093
2,19 / 4.	24,54	0,97	1670

### 2.3 Ocenjevnje kavitacije z vizualizacijo

Kavitacija je viden pojav, zato ga lahko opazujemo z računalniško vizualizacijo. Kavitacijski oblaki, ki so predmet raziskave, oblikujejo skalarna polja moči svetlobe v prostoru in času. S pomočjo časovno zaporedne digitalizacije slik so nastale posamezne sočasne časovne vrste, ki popisujejo kavitacijske sestave.

Za vsak kavitacijski režim sta bili posneti dve seriji 500 slik s frekvenco zajemanja slik 25 slik/s. Prva serija predstavlja pogled na krilo od zgoraj, druga pa s strani. Signal iz video kamere je bil digitaliziran s kartico za zajemanje slik s 24-bitno barvno ločljivostjo v sistemu M-JPEG. Za nadaljnjo uporabo in analizo v programu za vrednotenje dinamičnih pojavov na digitalnih slikah Dynascan [7] je bila ločljivost zmanjšana na 256 odtenkov sivine.

Statistično vrednoteno vidno polje je bilo razdeljeno na 225 oken (sl. 4). Pri pogledu od zgoraj je bila velikost vsakega okna  $15 \times 15$  točk, pri pogledu od strani pa je bilo okno veliko  $5 \times 5$  točk. Za vsako okno je bila izračunana skalarna funkcija [7]:

$$A(k, t) = \frac{1}{225} \sum_{l=1}^{15} \sum_{m=1}^{15} E(l, m) \dots \dots E(l, m) = \{0, 1 \dots 255\} \quad (2),$$

kjer  $E$  podaja lokalno,  $A$  pa povprečeno svetlost. Količinska ocena kavitacijske sestave na opazovanem območju krila v navpični in vodoravni smeri prečno na krilo je podana v obliki prostorskih topoloških porazdelitev skalarne funkcije:

$$\bar{A}(k) = \frac{1}{N} \sum_t A(k, t) \quad \text{and} \quad (3)$$

in

$$s(k) = \sqrt{\frac{1}{N-1} \sum_t \left( \bar{A}(k) - A(k, t) \right)^2}$$

kjer je  $\bar{A}(k)$  povprečna jakost in  $s(k)$  standardno odstopanje moči svetlobe.

Z enačbami (2) in (3) so bile ocenjene lokalne karakteristike topoloških sestavov kinematike kavitacijskega oblaka pri različnih celovitih parametrih kavitacije, ki so določeni s preglednico 1. Lego in vrednost največje moči kavitacije je mogoče oceniti s slike 5. Oba parametra se znatno spreminjata s celovitimi

### 2.3 Cavitation evaluation using the computer-aided visualization method

Cavitation is a visual phenomenon that can be observed with a computer-aided visualization method. The observed cavitation clouds form scalar patterns of grey-level intensity in space and time. With time-successive digitisation of the images, time series that describe the observed cavitation structures were generated.

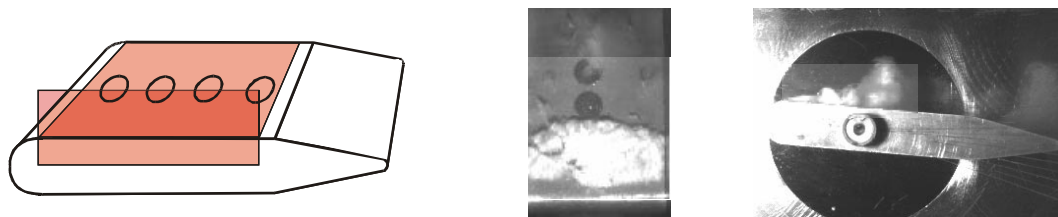
Five hundred images of the top and side view were recorded for each respective cavitation condition (cavitation number) with a sampling frequency of 25 images/s. The camera signal was digitized using an image-capturing card with a 24-bit colour resolution in the M-JPEG system. For further analyses with Dynascan software [7], for quantification of the dynamic phenomena of digital images, the resolution was decreased to 256 grey levels.

The region of interest for the statistical evaluation (Figure 4) was divided into 225 observation areas (windows). Each window had a size of  $15 \times 15$  pixels at the top view and  $5 \times 5$  pixels at the side view. For each window a scalar function was calculated [7]:

where  $E$  is the local grey-level intensity and  $A$  is the average grey-level intensity. A quantitative evaluation of the cavitation structure in the observed hydrofoil area in the vertical and horizontal directions perpendicular to the hydrofoil is given in the form of space-distributed topological structures of the scalar function:

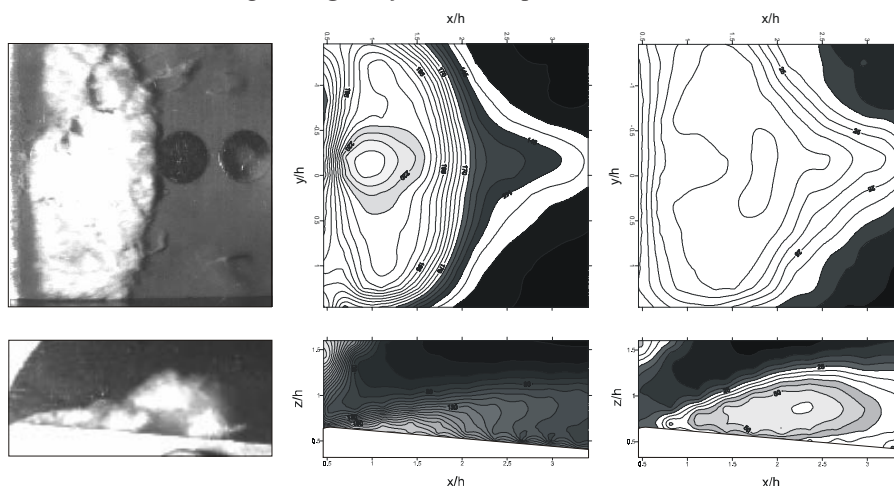
where  $\bar{A}(k)$  is the average and  $s(k)$  the standard deviation of grey-level intensity.

With equations (2) and (3) the local characteristics or topological structures of the kinematics of the cavitation cloud under different cavitation conditions, given in Table 1, were evaluated. The position and the value of the maximum cavitation intensity can be evaluated from Figure 5. Both parameters change significantly when the integral



Sl. 4. Lega opazovalnega polja pri pogledu od zgoraj in s strani

Fig. 4. Region of interest: top and side view



Sl. 5. Slike kavitacije (levo), pripadajoča srednja vrednost svetlosti ( $v$  v sredini) in standardno odstopanje vrednosti svetlosti (desno). Zgornja vrsta slik je pogled od zgoraj, spodnja pa s strani. Smer toka je od leve proti desni, hitrost toka  $v = 16$  m/s, natočni kot  $\delta = 5^\circ$  in kavitacijsko število  $\sigma = 2,4$ .

Fig. 5. Cavitation figures (left), distributions of average grey level (middle), distributions of the standard deviation of grey level (right). The upper row of figures is a ground plan, and the lower the sideview. The flow direction is from left to right, flow velocity  $v = 16$  m/s, angle of inclination  $\delta = 5^\circ$ , cavitation number  $\sigma = 2.4$ .

parametri kavitacije. Lega lokalnih kavitacijskih ekstremov podajata v brezdimenzijski obliki  $y/h$  in  $x/h$ , kjer sta  $x$  in  $y$  koordinati v poldnevni ravnini krila,  $h$  pa je debelina krila. Na sliki 6 so prikazane porazdelitve srednje vrednosti svetlosti in standardno odstopanje svetlosti pri nespremenljivem vpadnem kotu  $\delta = 5^\circ$  za štiri kavitacijska števila, podana v preglednici 1.

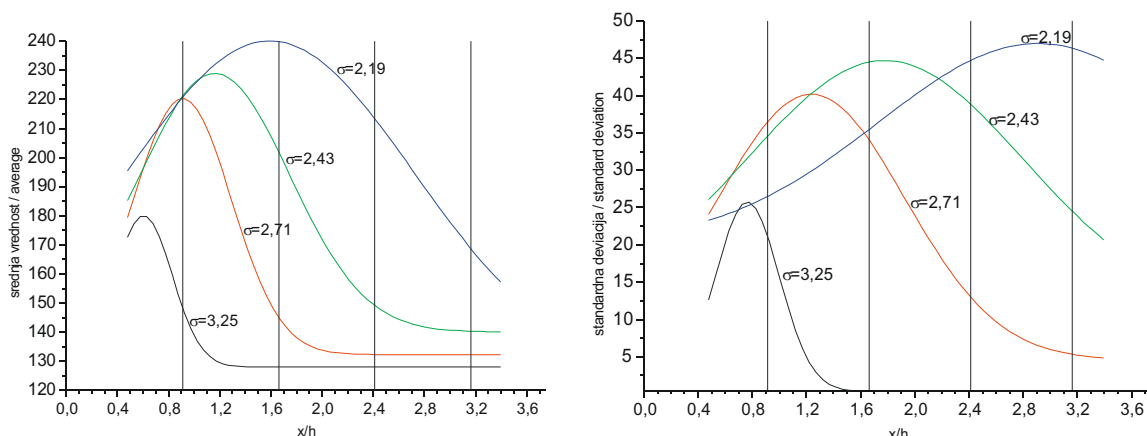
Srednja vrednost svetlosti  $A$  in standardno odstopanje svetlosti  $s$  pri nespremenljivem kavitacijskem številu  $\sigma$  popisujeta intenziteto kavitacije vzdolž krila. Moč kavitacije se povečuje vzdolž krila, doseže največjo vrednost in se zmanjša na prehodu ravnega dela krila v klinasto obliko krila. Lega in moč kavitacije, ki sta popisani s parametroma  $A$  in  $\sigma$  v odvisnosti od razdalje  $x/h$ , sta značilno odvisni od kavitacijskega števila  $\sigma$ . Z zmanjševanjem kavitacijskega števila  $\sigma$  se moč kavitacije povečuje, lega največjih vrednosti spremenljivk  $A$  in  $s$  pa se premika vzdolž krila.

Drug pomemben podatek o kavitacijskih razmerah na osamljenem krilu je odmik kavitacijskega oblaka od površine krila oziroma lega kavitacijskega oblaka nad krilom. Oddaljenost kavitacijskega oblaka od površine je določena iz diagramov lokalnih

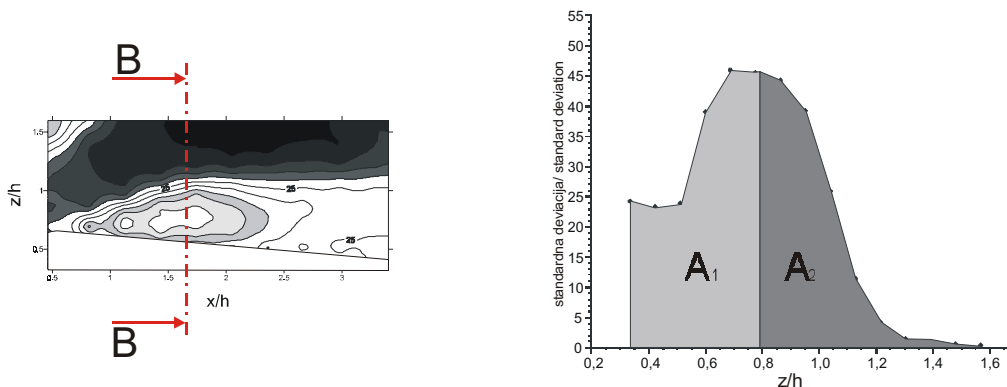
cavitation parameters are changed. The position of the local cavitation extremes is given in non-dimensional form,  $y/h$  and  $x/h$ , where  $x$  and  $y$  are the coordinates in the meridian plane of the hydrofoil, and  $h$  is the hydrofoil's thickness. Figure 6 shows the distribution of the average grey level and the standard deviation of the grey level at a constant inclination angle  $5^\circ$ , for four different cavitation numbers (Table 1).

The average grey level  $A$  and the standard deviation of the grey level  $s$  at constant cavitation number  $\sigma$ , describe the cavitation intensity along the hydrofoil. The cavitation intensity is increased along the hydrofoil in a streamwise direction, reaches its maximum value, and is decreased at the transition of the hydrofoil shape from straight to a wedge. The location and magnitude of the cavitation, described with the parameters  $A$  and  $\sigma$ , and their dependence on the distance  $x/h$ , are both dependent on the cavitation number  $\sigma$ . When  $\sigma$  is decreased, the cavitation intensity is increased, and the location of the maximum values of  $A$  and  $s$  is moved along the hydrofoil.

The second important parameter describing the cavitation conditions on the hydrofoil is the distance of cavitation cloud from the hydrofoil surface, i.e. its position above the hydrofoil. Its distance is determined from the side-view diagrams



Sl. 6. Srednja vrednost in standardno odstopanje svetlosti v odvisnosti od  $x/h$  za vse režime pri natočnem kotu  $\delta = 5^\circ$ . Pokončne črte označujejo mesta, kjer so nameščeni bakreni vzorci.  
 Fig. 6. Distributions of the average grey level and the standard deviation of the grey level versus  $x/h$  for all flow conditions at an inclination angle  $5^\circ$ . Vertical lines denote positions of copper specimens.



Sl. 7. Mesto prereza  $x/h$  nad drugim vzorcem za kavitacijsko število  $\sigma_2$  in diagram porazdelitve standardnega odstopanja  $\sigma$  pri nespremenljivi vrednosti  $x/h$  v odvisnosti od  $z/h$   
 Fig. 7. Position of section  $x/h$  for second specimen – cavitation number  $\sigma_2$ , and graph of standard deviation of grey-level distribution at a constant value  $x/h$  versus  $z/h$

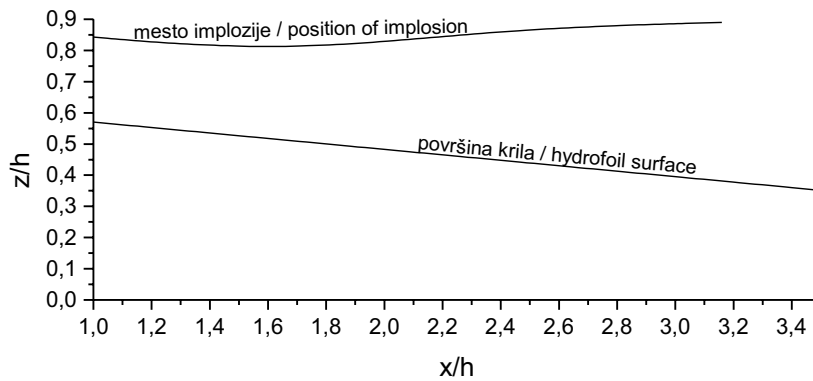
porazdelitev moč kavitacije pri pogledu s strani. Na sliki 7 je prikazana porazdelitev standardnega odstopanja svetlosti pri nespremenljivi vrednosti  $x/h$  v odvisnosti od  $z/h$ .

Za mesto implozije kavitacijskega oblaka je bila izbrana vrednost  $z/h$ , kjer je diagram porazdelitve standardnega odstopanja svetlosti  $s$  ploščinsko razdeljen na dva enaka dela ( $A_1 = A_2$ ) (sl. 7). Brezdimenzijska oddaljenost mesta implozije  $l$  kavitacijskega oblaka od površine krila je bila določena z razliko mesta implozije in brezdimenzijsko višino krila na tem mestu. Pri tem ni bil upoštevan vpliv strmine krila  $\delta$ . Mesto implozije kavitacijskega oblaka se pri nespremenljivem kavitacijskem številu  $\sigma$  vzdolž krila monotono odmika od površine krila, kar je posledica tokovnega polja okoli krila. Diagram mesta implozije kavitacijskega oblaka v odvisnosti od vrednosti  $x/h$  je prikazan na sliki 8.

of local cavitation intensity distributions. Figure 7 shows an example of the standard deviation distribution at a constant value  $x/h$  with its dependence on  $z/h$ .

The position of the cavitation-cloud implosion was determined with the value  $z/h$ , where the diagram of the standard deviation of the grey-level distribution  $s$  is divided into two areas of equal size ( $A_1 = A_2$ ), Figure 7. The non-dimensional distance  $l$  of the cavitation-cloud implosion from the hydrofoil surface is determined by the difference between the position of the cavitation implosion and a non-dimensional height of the hydrofoil at that position. Because of the negligible error, the influence of the inclination angle  $\delta$  was not taken into consideration. The position of the cavitation-cloud implosion along the hydrofoil, at constant cavitation number  $\sigma$ , is moved away from the surface of the hydrofoil, influenced by the flow field around the hydrofoil. Figure 8 shows a diagram of the position of the cavitation-cloud implosion versus  $x/h$ .





Sl. 8. Mesto implozije kavitacijskega oblaka v odvisnosti od vrednosti x/h  
 Fig. 8. Position of cloud implosion versus x/h

3 ANALIZA REZULTATOV

3 ANALYSIS OF RESULTS

Cilj raziskave je bila postavitve empiričnega - fenomenološkega modela odvisnosti med vizualnimi sestavami kavitacije nad krilom in izmerjenimi erozijskimi učinki na površini krila. Vizualne sestave kavitacije podajata standardno odstopanje svetlosti *s* (sl. 6) in mesto implozije kavitacijskega oblaka (sl. 7), erozijske učinke pa podatki iz preglednice 2.

Fenomenološki model temelji na predpostavki, da je jakost erozije sorazmerna moči spreminjanja kavitacijskega oblaka in obratno sorazmerna oddaljenosti kavitacijskega oblaka od površine krila. Intenziteto erozije izrazimo z  $A_d/A_{ref}$ . Napoved jakosti kavitacijske erozije za opazovani preskus podaja enačba:

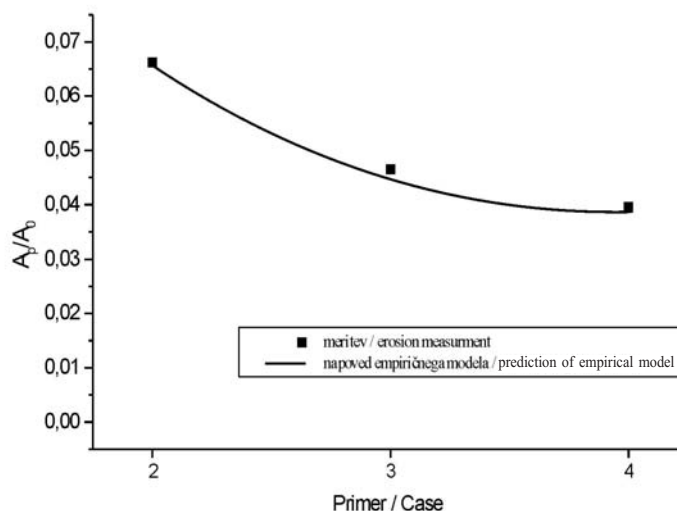
$$\frac{A_d}{A_{ref}} = 0,016443 \frac{s(k)^{0,070798}}{l^{0,898913}} \tag{4}$$

Koeficienti v enačbi (4) so določeni z metodo najmanjših kvadratov odstopanja, modeliranih iz izmerjenih vrednosti. Ujemanje napovedi modela z eksperimentalno izmerjenimi vrednostmi za vsa tri mesta čepov na krilu prikazuje slika 9.

The aim of the research was to establish an empirical-phenomenological model of the relation between the intensity of cavitation erosion on the hydrofoil surface and the visual cavitation structures above the hydrofoil. The visual cavitation structures are given by the standard deviation of the grey level *s* (Fig. 6) and by the position of the cavitation-cloud implosion (Fig. 7). The erosion effects are given by the data presented in Table 2.

The phenomenological model is based on a presumption that the erosion intensity is proportional to the fluctuation intensity of the cavitation cloud and inversely proportional to the distance of the cloud implosion from the hydrofoil surface. Erosion intensity is expressed by the ratio  $A_d/A_{ref}$ . The prediction of the intensity of cavitation erosion for the observed experiment is given by:

The coefficients in equation (4) are determined by the method of least squares for the deviation of the modelled and measured values. The agreement of the model prediction with the experimental values for all three specimen locations are presented in Figure 9.



Sl. 9. Primerjava napovedi modela in eksperimentalnih vrednosti erozije na vzorcih  
 Fig. 9. Comparison of the empirical model prediction and the experimental data of specimen erosion

## 4 SKLEP

V kavitacijskem predoru so bile pri izbranih celovitih karakteristikah izvedene meritve kavitacije na osamljenem krilu. Kavitacija na krilu je bila vrednotena z računalniško podprto vizualizacijo in z novo metodo za določanje kavitacijske erozije.

Na podlagi eksperimentalno dobljenih rezultatov kinematike kavitacijske sestave nad krilom in rezultatov erozije na opazovanih vzorcih površine krila je bil oblikovan pojavnostni model, ki napoveduje moč kavitacijske erozije.

Z razširitvijo študije na dejanska krila turbinskih strojev se odpira možnost oblikovanja pojavnostnih modelov napovedi erozije na rotorjih turbostrojev in uporabe računalniško podprte vizualizacije za opazovanje kavitacije na vodnih turbinah in velikih črpalkah.

## 5 ZAHVALA

V prispevku opisano raziskovalno delo je podprla Evropska komisija (Commission of the European Communities Directorate General for Energy and Transport) v okviru EU projekta 5. okvirnega programa: "Opazovanje kavitacije v hidravličnih strojih z računalniško podprto vizualizacijsko metodo (CAVISMONTOR)", št. pogodb: NNE5/1999/597.

## 4 CONCLUSIONS

In the cavitation tunnel we observed cavitation on the single hydrofoil at selected integral parameters. The cavitation was evaluated with the pit-count method and computer-aided visualization.

On the basis of the experimentally obtained results of the cavitation-structure kinematics above the hydrofoil, and the results of the erosion evaluation on the observed selected specimens of the hydrofoil surface, a phenomenological model was setup which predicts the magnitude of the cavitation erosion.

An expansion of the study to include real profiles of turbine machines opens up a possibility for developing phenomenological models for erosion prediction on turbomachinery rotors and the application of computer-aided visualization for cavitation monitoring on water turbines and large process pumps.

## 5 ACKNOWLEDGEMENTS

This research is supported by the Commission of the European Communities Directorate General for Energy and Transport, under the EU 5<sup>th</sup> Framework Project: "Cavitation Monitoring In Hydraulic Machines With Aid Of A Computer Aided Visualization Method (CAVISMONTOR)", Contract No. NNE5/1999/597.

6 LITERATURA  
6 REFERENCES

- [1] Young, F.R. (1999) Cavitation. *Imperial College Press*.
- [2] Hofmann, M. et al (1999) Numerical and experimental investigations on the self-oscillating behaviour of cloud cavitation - Part 1: Visualization.- V: *3<sup>rd</sup> ASME / JSME Joint Fluids Engineering Conference* (San Francisco, CA 1999).
- [3] Kern, I. (2000) Eksperimentalna raziskava dinamičnih parametrov na modelu Kaplanove vodne turbine, magistrsko delo, *Fakulteta za strojništvo*, Ljubljana.
- [4] Diodati, P., G. Giannini (2001) Cavitation damage on metallic plate surfaces oscillating at 20 kHz, *Ultrasonics Sonochemistry*, Volume 8, *Issue 1*, January 2001, 49-53.
- [5] Mann, B.S. (2000) High-energy particle impact wear resistance of hard coatings and their application in hydroturbines, *Wear*, Volume 237, *Issue 1*, January 2000, 140-146.
- [6] Pham, T.M., F. Larrarte, D. H. Furman (1999) Investigation of unsteady sheet cavitation and cloud cavitation mechanisms, *Journal of Fluids Engineering*, Transactions of the ASME, Volume 121, *Issue 2*, 289-296.
- [7] Širok, B., I. Kern, M. Hočevar, M. Novak (1999) Monitoring of the cavitation in the Kaplan turbine, *IEEE International Symposium on Industrial Electronics*, Volume 3, 1224-1228.
- [8] Okada, T., S. Hattori, M. Shimizu (1995) A fundamental study of cavitation erosion using a magnesium oxide single crystal (intensity and distribution of bubble collapse impact loads), *Wear*, Volumes 186-187, *Part 2*, August 1995, 437-443.
- [9] Caron, J.-F., M. Farhat, F. Avellan (1999) The influence of flow unsteadiness on erosive cavity dynamics, *Proceedings of the 1999 3rd ASME/JSME Joint Fluids Engineering Conference*, FEDSM'99, San Francisco, California, USA, 18-23 July (CD-ROM), *Published by American Society of Mechanical Engineers*, ISBN 0791819612, 1.

Naslovi avtorjev:

prof.dr. Brane Širok  
Matevž Dular  
dr. Marko Hočevar  
Univerza v Ljubljani  
Fakulteta za strojništvo  
Aškerčeva 6  
1000 Ljubljana  
brane.sirok@fs.uni-lj.si  
marko.hocevar@fs.uni-lj.si

dr. Matej Novak  
Turbonštitut  
Rovšnikova 7  
1210 Ljubljana  
matej.novak@turboinstitut.si

prof.dr. Bernd Stoffel  
dr. Gerhard Ludwig  
Bernd Bachert  
Darmstadt University of Technology  
Chair of Turbomachinery and Fluid Power  
Magdalenenstrasse 4  
D-64289 Darmstadt, Germany  
stoffel@tfa.machinenbau.tu-darmstadt.de  
ludwig@tfa.machinenbau.tu-darmstadt.de  
bachert@tfa.machinenbau.tu-darmstadt.de

Authors' Addresses:

Prof.Dr. Brane Širok  
Matevž Dular  
Dr. Marko Hočevar  
University of Ljubljana  
Faculty of Mechanical Engineering  
Aškerčeva 6  
1000 Ljubljana, Slovenia  
brane.sirok@fs.uni-lj.si  
marko.hocevar@fs.uni-lj.si

Dr. Matej Novak  
Turbonštitut  
Rovšnikova 7  
1210 Ljubljana  
matej.novak@turboinstitut.si

Prof.Dr. Bernd Stoffel  
Dr. Gerhard Ludwig  
Bernd Bachert  
Darmstadt University of Technology  
Chair of Turbomachinery and Fluid Power  
Magdalenenstrasse 4  
D-64289 Darmstadt, Germany  
stoffel@tfa.machinenbau.tu-darmstadt.de  
ludwig@tfa.machinenbau.tu-darmstadt.de  
bachert@tfa.machinenbau.tu-darmstadt.de

Prejeto: 7.2.2002  
Received:

Sprejeto: 20.9.2002  
Accepted: